applied sciences

MDPI

Article

Fluorescence Properties of the Air- and Freeze-Drying Treatment on Size-Fractioned Sediment Organic Matter

Cheng-Wen Chuang, Wei-Shiang Huang, Yung-Yu Liu, Chi-Ying Hsieh and Ting-Chien Chen *

Department of Environmental Science and Engineering, National Pingtung University of Science and Technology, Pingtung 91201, Taiwan; a0921765948@yahoo.com.tw (C.-W.C.); stefsun921015@gmail.com (W.-S.H.); uny10331099@gmail.com (Y.-Y.L.); chiying@mail.npust.edu.tw (C.-Y.H.)
* Correspondence: chen5637@mail.npust.edu.tw; Tel.: +886-8-774-0333; Fax: +886-8-774-0244

Abstract: Sediment humic substance (SHS) is a highly heterogeneous and complex organic mixture with a broad molecular weight range. It is the significant component that associates distribution, transport, and biotoxicity of pollutants in a river environment. Air- and freeze-drying sediment pre-treatment may cause different biological activity and may result in different chemical quantities and sediment organic matter. This study collected sediments that received livestock wastewater discharge. The sediments were air- (AD) and freeze-dried (FD). The dried sediment organic matter was extracted with an alkaline solution and separated into three size-fractioned SHS samples. Size-fractioning is an effective method used to differentiate materials, on a molecular level. The bulk solution (<0.45 μm) was designated as BHS, and size-fractioned solutions were identified as LHS (<1 kDa), MHS (1–10 kDa), and HHS (10 kDa–0.45 μm). The AD SHS had a lower dissolved organic carbon (DOC) concentration than the FD SHS for the bulk and individual size-fractioned SHS, but the AD and FD SHS had a similar distribution of organic carbon in the size-fractioned SHS. The AD SHS had higher aromaticity ($SUVA_{254}$) and an extent of humification (HIX) than the FD SHS. In addition, the high molecular weight SHS (HHS) had a higher $SUVA_{254}$ but lower HIX than the MHS and LHS. The HHS had significantly lower fulvic acid but had higher humic acid-like substances than the MHS and LHS. This is possibly the reason the LHS had a higher humification degree but lower aromaticity than HHS. The size-fractioned SHS and optical indicators distinguished the difference between the chemical properties when air- or freeze-dried, due to the different degree of biological activities.

Keywords: sediment humic substances; size-fractioned; optical indicators; air drying; freeze-drying

Citation: Chuang, C.-W.; Huang, W.-S.; Liu, Y.-Y.; Hsieh, C.-Y.; Chen, T.-C. Fluorescence Properties of the Air- and Freeze-Drying Treatment on Size-Fractioned Sediment Organic Matter. *Appl. Sci.* **2021**, *11*, 8220. https://doi.org/10.3390/app11178220

Academic Editors: Anna Annibaldi and Vlasoula Bekiari

Received: 18 June 2021
Accepted: 1 September 2021
Published: 4 September 2021

1. Introduction

Sediment dissolved organic matter (DOM) plays an essential role in the global biogeochemical cycling of carbon and nutrients [1,2]. The chemical properties of the sediment humic substance (SHS) are dynamic and are affected by environmental conditions and the source of organic matter [3–5]. Moreover, SHS is a highly heterogeneous and complex organic mixture with a broad molecular weight range [5]. The chemical structure and composition of SHS and the molecular weight are significant properties that associate pollutants distribution, transport, and biotoxicity in an aquatic environment [6–10]. High molecular weight DOM and SHS have high specific surface areas and form aggregated structures by inter- or intra-molecular interactions within the DOM and SHS. The properties provide the particular sorption sites for hydrophobic organic compounds and heavy metals [6,8,9,11–14]. However, other studies also reported low molecular weight DOM having significant sorption capacity for organic pollutants and heavy metals [15–18]. The chemical structure and composition of SHS and DOM might be the significant factor that influences the pollutants distribution, transport, and binding capacity [3,6,18–21].

Fluorescence and ultraviolet spectroscopy are sensitive and fast techniques that are widely used to investigate the composition and structure of SHS [11,22–25]. The aromaticity index ($SUVA_{254}$) and the humification index (HIX) have been widely employed to

investigate the chemical properties of DOM and SHS [2,5,9,10,18,19]. Moreover, the fluorescence regional integration (FRI) method divides the excitation and emission matrix (EEM) into five regions and utilizes the fluorescence intensity at all EEM wavelength pairs for sample characterization [22,26–28]. The FRI has been successfully and extensively utilized to characterize DOM in water and SHS in sediment and soil samples [27–30]. The optical indicators and FRI-coupled EEM technology are time-saving and require minimal sample pre-treatment compared with typical physicochemical methods [22,27,31].

Additionally, collected sediment generally has been pre-treated with air-drying (AD) or freeze-drying (FD). These two pre-treatment methods have resulted in different SHS quantities and qualities [10,32–34], due to biological activity. Shi et al. [10] reported that AD pre-treated sediment had slightly lower pH, organic matter, and total organic carbon compared to the FD pre-treated sediment. Since the SHS is a complex organic mixture with a wide-range molecular weight, size-fractioned SHS can be used as an effective method to investigate the differences between the chemical properties of SHS pre-treated by AD and FD [10]. This study investigated the SHS extracted from river sediment; it was pre-treated with both AD and FD methods. The extracted bulk SHS solution was separated into three size fractions. The bulk and size-fractioned SHS quantities were measured with dissolved organic carbon (DOC) concentrations, and the chemical characteristics were analyzed with UV-Vis and fluorescence spectroscopy. The indicators $SUVA_{254}$ and HIX were used to distinguish aromaticity and the extent of humification of the bulk and size-fractioned SHS. The chemical composition of the size-fractioned SHS was investigated with the FRI method.

2. Materials and Methods

2.1. Sediment Collection and Treatment

The studied sediment was collected from a sampling site (22°46′04.2″ N, 120°32′32.7″ E) in southern Taiwan, 50 m downstream of an animal wastewater discharge outlet. Water containing high concentrations of organic matter has been reported [9]. Livestock wastewater often contains high concentrations of particulate and dissolved organic matter which, when deposited on sediment, may cause a high level of organic matter in the sediment.

The sampling time for this study was from July to August 2011. Samples were taken once a week and a total of three samples were taken as triple samples for each drying method. The sediment sample collection used a stainless-steel sampling long dipper to take the surface sediment (0–15 cm). Each sampling used a simple, random sampling method to take the three sediment samples; the samples were mixed evenly into one sample. Each sample was about 2 kg and packed into a wide-mouth brown bottle for individual drying.

After the sediment was sent back to the laboratory, the sediments, which were to be air-dried, were spread on a plastic tray and placed in an area away from direct sunlight. The average outdoor temperature was 27 ± 2 °C. During the drying period, the sediments were flipped from time to time to evenly expose the sediments to the air. Due to the high temperature, we estimated that the sediment was dry within a month. The other sediment samples were freeze-dried (FD) immediately and the FD samples were then stored in a 4 °C refrigerator for one month.

The freeze- and air-dried samples were sieved with stainless-steel mesh (<2 mm). The sieved samples were then analyzed for basic properties, such as pH, total organic carbon (TOC), and organic matter, and stored in sealed plastic cans for subsequent tests. The dried sediments were passed through a 100-mesh (0.149 mm) sieve and one gram of the sieved sediment was analyzed with a solid TOC analyzer (1030S TOC Solids Module, O.I. Analytical) to quantify the TOC content in the sediment. To quantify the organic matter, one gram of sieved sediment was placed into a crucible, which was placed in the furnace (500 °C for 3 h). After cooling, the crucible was weighed. The organic matter content (%) = (weight lost by burning)/(weight of dried sediment) × 100%.

The extraction and purification of the SHS samples followed the procedure recommended by the International Humic Substances Society (IHSS) [6,35]. A 0.1 N HCl solution was added to remove the alkaline earth metals and carbonate. The residual sediment was

mixed with a 0.1 N NaOH solution at a ratio of 1/20 (*w*/*v*). The extracted NaOH solution was centrifuged (4500 rpm, 20 min) to separate the SHS, and then passed through a 0.45 µm filter (Pall) to collect the bulk SHS (BHS) solution, which was at an alkaline pH. Sodium azide (0.5%) was added to the BHS solution to prevent bacterial growth and then stored in a 4 °C refrigerator. To avoid contamination of the container, it was previously washed with ultrapure water.

2.2. SHS Size Separation

In each separation process, three liters of the extracted BHS solution (<0.45 µm) were separated into three size-fractioned samples: 10 kDa < HHS < 0.45 µm, 1 kDa < MHS < 10 kDa, and LHS < 1 kDa using cross-flow ultrafiltration equipment with a ceramic membrane (Filtanium, France, cut-off pore size of 10 and 1 kDa, membrane area of 320 cm^2). The concentration factor was kept at 10 (ratio of feed volume divided by retentate volume). The volume fractions were 1.0, 0.1, 0.09, and 0.81 for the BHS, HHS, MHS, and LHS, respectively. The feed flow rate was 1.7–2.0 L/min and penetrant flow rates were 12 and 25 mL/min for the 10 kDa and 1 kDa membranes, respectively. The feed flow pressure for the separation process was 5 kg/cm^2. The BHS and the three size-fractioned SHS samples measured DOC concentration, UV/Vis, and fluorescence spectroscopy.

2.3. UV/Vis Measurements

An aliquot of 5 mg-C/L from each of the four SHS solutions was measured with a UV/Vis spectrophotometer (Hitachi, U-2900, Tokyo, Japan) for absorbance, at a scanning wavelength of 800–200 nm. Before the measurement, the SHS solutions were adjusted to pH 7 with 0.3 N H_2SO_4. The background was corrected per the Helms et al. [36] method. The UV/Vis indicator $SUVA_{254}$ (L/mg-C/m) = $(UV_{254}/(HS)) \times 100$, where UV_{254} was the UV/Vis absorbance at 254 nm (cm^{-1}) of the sample, and (HS) was the DOC concentration (mg-C/L) of the SHS solution [24,37]. The other UV/Vis indicators, $S_{275–295}$, S_R ($S_{275–295}/S_{350–375}$), and $A_{250–400}$ were also analyzed. However, these indicators were not significantly different between the AD and FD samples; they are not discussed in the present study and the $S_{275–295}$, S_R, and $A_{250–400}$ data are listed in the Supplementary Information (Table S1).

2.4. Fluorescence Spectroscopy and Fluorescence Region Integration (FRI)

An aliquot of 5 mg-C/L for each of the four SHS solutions was measured by a fluorescence spectrophotometer (Hitachi, F-7000). The three-dimensional fluorescence excitation/emission matrix (EEM) was recorded. Before the measurement, the SHS solutions were adjusted to pH 7 with 0.3 N H_2SO_4. Fluorescent scanning used an excitation wavelength of 200–450 nm with 5 nm increments and an emission wavelength of 250–550 nm with 2 nm increments. The scan rate was 2400 nm/min, the slit width was 5 nm, and the voltage amplification was 700 V. The spectra were obtained by subtracting an ultrapure water blank spectrum, recorded in the same conditions, to eliminate the Raman scatter peaks. The HIX was calculated when the excitation wavelength was 254 nm. The sum of the emission wavelength at 435–480 nm was divided by the sum of the emission wavelength at 300–345 nm [38] as in Equation (1). The other fluorescence indexes (biological index (BIX) and fluorescence index (FI)) were also analyzed in the present study. These indicators were not significantly different between the AD and FD samples; they are not discussed in the study and the BIX and FI data are listed in the Supplementary Information (Table S1).

Fluorescence region integration (FRI) is a quantitative analysis tool that divides the EEM into five regions and utilizes the fluorescence intensity at all excitation-emission wavelength pairs for sample characterization [22,27,28]. The percentage of fluorescence response ($P_{i,n} = \Phi_{i,n}/\Phi_{T,n}$) was calculated according to Chen et al. [22] and Tian et al. [27],

where $\Phi_{i,n}$ and $\Phi_{T,n}$ were the normalized excitation–emission area volumes referring to the value of region i and the entire region, respectively.

$$\text{HIX} = \frac{\text{E}_\text{m} = 435 - 480\ \text{nm}}{\text{E}_\text{m} = 300 - 345\ \text{nm}} \text{ at } \text{E}_\text{x} = 254\ \text{nm} \quad (1)$$

2.5. Statistical Analysis and Calculation of Fluorescence Data

In this study, using the R software (2.13.2 V) to calculate fluorescent and UV/Vis indicators, the EEM analysis and plots followed a modified R script developed by Lapworth and Kinniburgh [39]. Linear regression, difference, and *t*-test used the S-Plus software (V 6.2). The difference test used the ANOVA test method for the three SHS solutions and the *t*-test method was used for the two-group data at significance levels ($p < 0.05$).

3. Results and Discussion

3.1. DOC Concentrations and Carbon Mass Fractions of the Size-Fractioned SHS

The basic properties of the AD- and FD-treated sediments are listed in Table 1. The AD and FD pH values were within neutral values, ranging from 6.63 to 7.25. The average FD pH value was significantly higher than the AD value ($p = 0.017$). The FD organic matter (OM) and TOC concentrations were higher than the AD but insignificantly different ($p = 0.62$ and 0.51, respectively).

Table 1. Basic sediment properties in AD and FD samples.

Sample	pH	TOC (g/kg)	OM (%)	TOC/OM (%)
AD	6.78 ± 0.17 *	44.1 ± 11.0	7.45 ± 1.1	58.8 ± 12.1
FD	7.19 ± 0.05	50.4 ± 11.0	7.92 ± 0.9	64.2 ± 15.0

* indicated $p < 0.05$.

The DOC concentration is a standard parameter of natural organic matter and SHS [1,40]. The DOC concentrations of the bulk SHS (BHS) sample and the three size-fractioned SHS samples are listed in Table 2. The BHS DOC concentrations (323–440 mg-C/L, average 7.36 g-C/kg based on sediment mass) of the FD sample were significantly higher than the AD sample (190–213 mg-C/L, average 4.02 g-C/kg based on sediment mass) ($p = 0.011$). The readily biodegradable and labile organic matter experienced oxidation cleavage that mineralized to carbon dioxide and generated organic acid via biodegradation in the AD process [4,41]; hence, the AD sediment had a lower pH value, OM, and TOC concentrations, and BHS had lower DOC concentrations than the FD samples.

Table 2. DOC concentrations (mg-C/L) of extracted size-fractioned HS in AD and FD samples.

Sample	BHS *	HHS *	MHS *	LHS *
AD	201 ± 12	1203 ± 102	445 ± 83	28.2 ± 3.9
FD	368 ± 63	2455 ± 576	915 ± 186	56.9 ± 11.5

* measured DOC concentrations.

The FD DOC concentrations were significantly higher in each size-fractioned SHS sample than the AD samples ($p < 0.02$). The overall organic carbon recoveries between the size-fractioned SHS and BHS samples were 91.3 ± 1.9% (AD) and 101.3 ± 6.1% (FD), which were within a reasonable range (100 ± 25%) [42]. The percent contribution of each size-fractioned solution to the total DOC concentration of the overall BHS solutions was 65.7 ± 4.3%, 21.9 ± 4.1%, and 12.4 ± 1.1% for HHS, MHS, and LHS, respectively, for the AD samples and was 65.4 ± 2.4%, 22.2 ± 1.2%, and 12.6 ± 3.5% for HHS, MHS, and LHS, respectively, for the FD samples. The two pre-treatment drying methods had no carbon mass fraction difference ($p = 0.93$–0.97). The organic carbon mass fractions of each size-fractioned SHS sample were not significantly different, which suggested that the

sediment OM was diagenetically uniform within the AD and FD treatments. The SHS carbon mass for the high molecular weight fraction (>1 kDa) averaged 87%, which was higher than the surface water systems' carbon mass fraction, which ranged from 20% to 67% [2,34–45]. It was also higher than the water extracted organic matter (WEOM) from the sediment's carbon mass fractions, ranging from 52% to 53% [3]. The organic carbon mass fraction of the high molecular weight fraction was comparable to the alkaline-extracted SHS solutions from sediments and ranged from 78% to 85% [9,10,17]. The sediment particular organic matter experienced hydrolysis and/or oxidative cleavage, starting with the low molecular weight and labile organic matter [4]. The exchange process of particulate and dissolved organic matter left high molecular weight organic matter in the sediment; hence, the alkaline-extracted SHS had a higher percentage of the high molecular weight carbon mass fraction.

3.2. Optical Indices of SHS

Precise UV/Vis and fluorescent analysis can obtain valuable DOM information [24,36,37,40,46,47]. In this study, the specific ultraviolet absorbance at wavelength 254 nm ($SUVA_{254}$) and the humification index (HIX) was used to analyze the chemical properties of the bulk and size-fractioned SHS samples. The $SUVA_{254}$ and HIX of the bulk and size-fractioned SHS for the AD and FD samples are shown in Figure 1a,b. The $SUVA_{254}$ value is a surrogate for the abundance of aromaticity for SHS [12,24,37]. The HIX is an indicator of material age and recalcitrance. HIX has been widely applied to investigate the extent of humification in SHS [11,48]. The $SUVA_{254}$ and HIX values were 1.98 ± 0.51 L/mg-C/m and 2.10 ± 0.30, respectively, of the total SHS solutions, which were lower than the average values of 4.2 ± 1.9 L/mg-C/m ($SUVA_{254}$) and 5.45 ± 3.80 (HIX) of the alkaline-extracted SHS samples taken from 43 stream sediments [5]. The $SUVA_{254}$ and HIX values were comparable to the alkaline-extracted SHS samples measured in sediments taken from a lake, industrial water, and a stream [6,10,20].

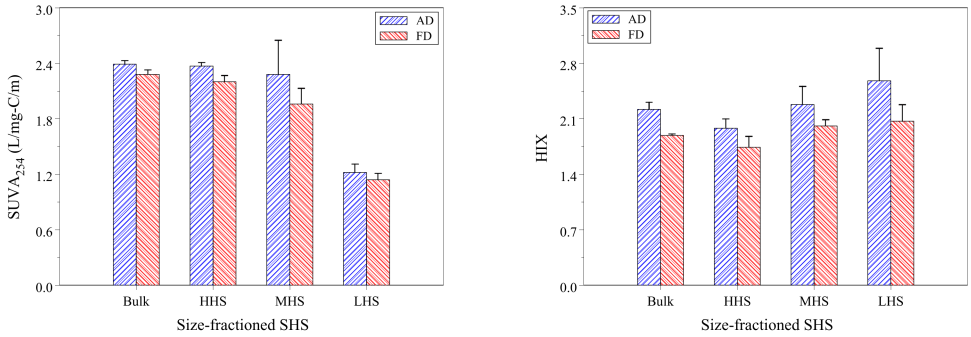

Figure 1. (**a**,**b**) Optical indicators varied with size-fractioned AEOM for AD and FD samples.

The $SUVA_{254}$ and HIX values of the AD bulk SHS were significantly higher than the FD bulk SHS (p = 0.047 and 0.018, respectively). In individual size-fractioned SHS samples, the $SUVA_{254}$ and HIX values of the AD samples were higher than the values of the FD samples, though insignificantly different (except the $SUVA_{254}$ of HHS). The high $SUVA_{254}$ and HIX values implied that the AD treatment had developed more aromatic functional groups and recalcitrant humic-like substances than the FD treatment due to biological activity. In the HHS samples, the average AD $SUVA_{254}$ value was significantly higher than the FD samples (p = 0.02), consistent with the fluorescence regional integration (FRI) results.

We compared the indicator difference between the size-fractioned SHS samples; for each sized SHS sample, the AD and FD samples were combined as a pooled sample. The average $SUVA_{254}$ values were 2.29 ± 0.11 and 2.12 ± 0.31 L/mg-C/m for HHS and MHS, respectively, which were significantly higher than the average LHS value of

1.18 ± 0.08 L/mg-C/m ($p < 0.001$) (Figure 1a). However, the HIX values were 1.86 ± 0.18, 2.15 ± 0.22, and 2.33 ± 0.40 for HHS, MHS, and LHS, respectively. The LHS HIX values were significantly higher than the HHS HIX values ($p = 0.036$) (Figure 1b). Most studies have shown high molecular weight SHS with a high HIX [9,19]; however, sediment low molecular weight water extracted organic matters (WEOM) had a higher HIX value than observed with the high molecular weight [3]. The SHS composition may cause these reverse conditions. The $SUVA_{254}$ values of all samples were <3.0, which suggested that the SHS composition was predominantly a hydrophilic substance with poor aromaticity [40]. The HIX values of all samples were <4, which suggested the SHS was of biological or aquatic origin with a low degree of humification [23,49]. The SHS composition characteristics were further examined with the FRI method as shown in Section 3.3.

3.3. Fluorescence EEM and Fluorescence Regional Integration (FRI)

A fluorescence spectroscope is a sensitive monitoring tool. The EEMs had similar patterns for each size-fractioned SHS, for both the AD and FD samples. Figure 2d shows 3D EEM plots for AD BHS, HHS, MHS, and LHS samples at 5 mg-C/L DOC of AD samples. The corrected EEMs were analyzed using an FRI technique developed by Chen et al. [22]. The EEM was separated into five excitation-emission regions relating to simple aromatic proteins (Regions I and II, E_x/E_m = 200–250/280–330 nm for region I, E_x/E_m = 200–250/330–380 nm for region II), fulvic acid-like materials (Region III, E_x/E_m = 200–250/380–520 nm), soluble microbial by-product-like materials (Region IV, E_x/E_m = 250–440/280–380 nm), and humic acid-like compounds (Region V, E_x/E_m = 250–440/380–520 nm) [22,27,31]. The $P_{V,n}$ percentage of the AD HHS samples was significantly higher than the FD HHS samples (Table 3).

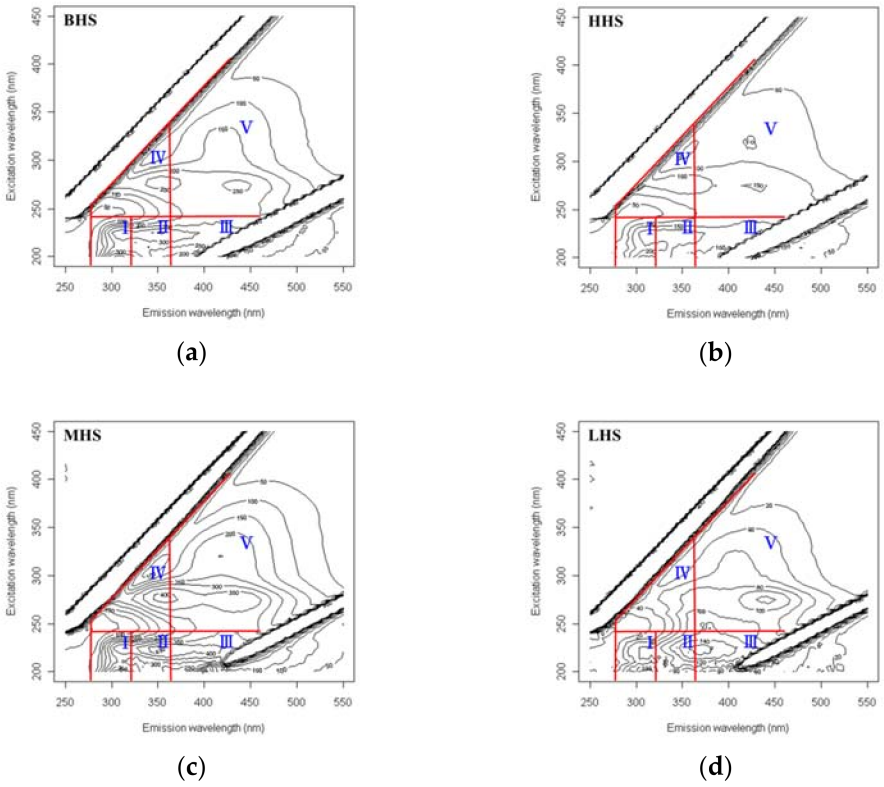

Figure 2. EEM diagrams of bulk and size-fractioned SHS with the air-dry method and the FRI regions: (**a**) BHS, (**b**) HHS, (**c**) MHS, and (**d**) LHS.

Table 3. Percentages of fluorescence region integration (FRI) among HHS, MHS, and LHS of the AD and FD samples.

Sample	$P_{I,n}$ (%)	$P_{II,n}$ (%)	$P_{III,n}$ (%)	$P_{IV,n}$ (%)	$P_{V,n}$ (%)
AD_{BHS}	18.3 ± 0.9	22.0 ± 0.3	23.7 ± 0.2 *	15.7 ± 0.4	20.1 ± 0.6
FD_{BHS}	19.3 ± 0.3	22.7 ± 0.1	22.1 ± 0.2	16.6 ± 0.3	19.3 ± 0.1
AD_{HHS}	18.8 ± 0.1 *	20.8 ± 0.3	21.2 ± 0.6	18.5 ± 0.9	20.7 ± 0.1 *
FD_{HHS}	20.1 ± 0.3	21.4 ± 0.3	20.0 ± 0.6	19.0 ± 0.5	19.5 ± 0.3
AD_{MHS}	18.9 ± 1.0	24.8 ± 0.6	26.1 ± 1.0	11.5 ± 0.5	18.6 ± 0.6
FD_{MHS}	20.5 ± 0.8	25.6 ± 0.5	25.3 ± 0.6	10.9 ± 0.2	17.6 ± 0.7
AD_{LHS}	14.7 ± 0.8 *	25.9 ± 2.4	29.8 ± 0.8 *	11.2 ± 0.4	18.4 ± 2.5
FD_{LHS}	16.5 ± 0.6	26.3 ± 0.6	27.7 ± 0.8	11.6 ± 0.5	17.8 ± 0.7

* significant difference ($p < 0.05$) between the ADS and FDS samples.

Table 3 shows the percentages of the five regions for both the AD and FD samples in bulk and three size-fractioned SHS samples. The percentages of $P_{I,n}$, $P_{II,n}$, and $P_{IV,n}$, in the FD samples were higher than in the AD samples (except the $P_{IV,n}$ of MHS), but the percentages of $P_{III,n,}$ and $P_{V,n}$ in the FD samples were less than the AD samples for the bulk and individual size-fractioned SHS samples. Fluorophores in the $P_{I,n}$, $P_{II,n}$, and $P_{IV,n}$ regions are attributed to microbial and aquatic sources. The average biochemical fraction (Bio = PI,n + PII,n + PIV,n) of the AD samples (55.3 ± 2.9%) was lower than the FD samples (57.6 ± 2.5%) [50,51]. In the PV,n and PIII,n regions, the fluorophores can be attributed to the humic acid- and fulvic acid-like substances. The average geochemical fraction (Geo = PIII,n + PV,n) of AD samples (44.7 ± 2.9%) was higher than the FD samples (42.4 ± 2.5%). The composition dissimilarity of the AD and FD samples could be due to a continual biochemical reaction in the sediment organic matter of the AD process, which would increase the ratio of long-wavelength pair fluorophores in the AD sample [50,51]. The $P_{V,n}$ percentage of HHS in the AD samples was significantly higher than in the FD sample ($p = 0.005$), consistent with the considerably higher $SUVA_{254}$ value of the AD samples in HHS (Figure 1a).

Figure 3 shows the percentage of each region for the three size-fractioned SHS samples when the AD and FD samples were combined as a pooled sample. The HHS and MHS had higher $P_{I,n}$ ratios than LHS ($p = 0.003$), but HHS had a lower $P_{II,n}$ ratio than MHS and LHS ($p = 0.003$). The $P_{I,n}$ region is located at a short emission wavelength having loose, simple aromatic proteins. The $P_{II,n}$ region is located relative to a long emission wavelength having condensed simple aromatic proteins [52,53]. The HHS had a relatively high, short emission wavelength protein-like substance, but LHS had a relatively high, long emission wavelength protein-like substance. In addition, the HHS had higher ratios of $P_{IV,n}$ than MHS and LHS ($p < 0.001$). The HHS Bio percentages (59.3 ± 1.5%) were significantly higher than the LHS (53.1 ± 2.8%) ($p = 0.002$). The LHS had a higher $P_{III,n}$ ratio than HHS ($p < 0.001$), which demonstrated that LHS had a higher fulvic acid-like substance content than HHS and MHS. The HHS had higher ratios of $P_{V,n}$ than MHS and LHS ($p = 0.013$). $P_{V,n}$ percentage is a fraction of the humic acid-like substance. The percentages of FRI show that HHS had a high humic acid-like substance, but LHS had a high fulvic acid-like substance. The $P_{III,n}$ and $P_{V,n}$ fractions can be attributed to the Geo fractions; the HHS Geo percentages (40.7 ± 1.5%) were significantly lower than LHS (46.9 ± 2.8%) ($p = 0.002$). The HHS's high Bio and low Geo fractions reflected that the HHS had lower HIX values than LHS (Figure 1b).

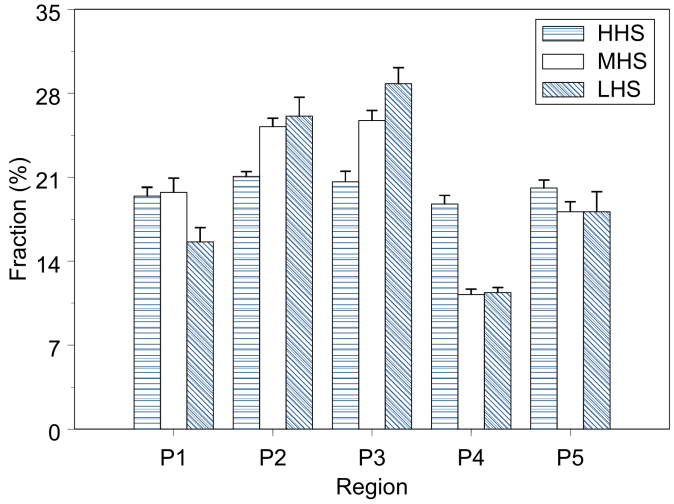

Figure 3. FRI percentages of size-fractioned SHS considering the AD and FD samples as pooled samples.

The $SUVA_{254}$ and HIX had a negative correlation (r = −0.41, $p = 0.049$). The $SUVA_{254}$ had a significantly positive correlation with the percentage of Bio fractions (r = 0.64, $p < 0.001$), but the HIX had a significantly positive correlation with the percentage of Geo fractions (r = 0.93, $p < 0.001$).

The river water received livestock wastewater containing a great amount of low humification particulate organic matter (POM). The POM that was deposited in the sediment suffered anaerobic biochemical oxidation, which resulted in low aromaticity and low humification in the sediment organic matter. The hydrolysis and oxidation cleavage processes in an anaerobic sediment environment favored decomposing low molecular weight and labile POM [1,4]. The remaining low molecular weight SHS in sediment, after hydrolysis and oxidation cleavage, greatly increased humification compared to the high molecular weight SHS. The HIX significantly correlated with fulvic acid-like (r = 0.76, $p< 0.001$) and geochemical fractions. The $SUVA_{254}$ values (Figure 1a) suggested that the bulk and size-fractioned SHS attributed to the hydrophilic aromatic substances; this implied that the sediment organic matter did not develop abundant aromaticity. The biochemical fraction that influenced the $SUVA_{254}$ values strongly correlated with the Bio fraction, which suggested aromaticity in the SHS in the present study sediment.

Besides the percentages of FRI fractions, the present study investigated FRI ratios $P_{III,n}/P_{II,n}$ for the size-fractioned SHS. The PIII,n/PII,n ratios were 1.11 ± 0.11 (LHS) > 1.02 ± 0.06 (MHS) > 0.98 ± 0.05 (HHS) and had a significantly positive correlation with the HIX (r = 0.96, $p< 0.001$, Figure 4). The $P_{III,n}/P_{II,n}$ ratios reflected the extent of humification of water extracted organic matter (WEOM) and SHS, which has been observed in suspended particulate matter (SPM) and sediments [54]. Wang et al. [54] reported the WEOM EEM component (C2/C3) ratios were 0.69 ± 0.03 for sediment and 1.15 ± 0.04 for SPM. The C2/C3 ratios had a positive correlation with the HIX. The C2 is located at E_x/E_m = 270/460 nm and C3 is located at E_x/E_m = 220/340 nm, which are located at regions V and II, respectively. The C2 excitation wavelength was close to the border (250 nm) of regions V and III, such that the peak (C2) may have properties close to the fulvic acid-like substance (PIII,n). The C3 is attributed to protein-like (PII,n) substances. In the present study, the LHS had higher PIII,n/PII,n ratios than HHS, and the PIII,n/PII,n ratios had a strong positive correlation with the HIX. The high HIX values in LHS are attributed to the composition of protein- and fulvic acid-like substances compared to HHS. Moreover, the $P_{III,n}/P_{II,n}$ ratio of AD (1.08 ± 0.08) was significantly higher than FD (0.99 ± 0.06, $p = 0.006$). The ratios had a significantly negative correlation with the $SUVA_{254}$ (r = −0.46, $p = 0.024$) for the total SHS (Figure 4). However, when the SHS was separated into two groups, LHS and the other group, which included BHS, HHS, and MHS, the $SUVA_{254}$ had an insignificant correlation with the $P_{III,n}/P_{II,n}$ ratios for both SHS groups (r = 0.17–0.19,

Figure 4). This suggested that the SHS aromaticity was not developed to the extent of the humification in SHS. The HHS and MHS had a higher $SUVA_{254}$ and $P_{V,n}$ percentage than LHS. One possible reason is that the HHS contains aromatic lignin resulting from the POM.

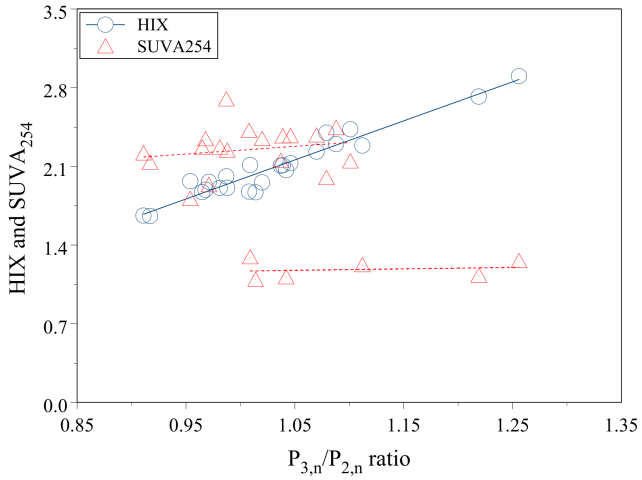

Figure 4. The linear correlation of optical indicators HIX and $SUVA_{254}$ with $P_{III,n}/P_{II,n}$.

4. Conclusions

In this study, SHS was extracted from surface sediment that contained organic matter discharged from livestock wastewater. The AD samples had a lower pH value, TOC, and OM level, which could be due to the mineralization of readily biodegradable OM in the AD process. The DOC concentrations of the AD SHS were significantly lower than the FD SHS, but the OC mass fractions of the size-fractioned SHS were insignificantly different between the AD and FD SHS. The $SUVA_{254}$ and HIX reflected a low degree of aromaticity and humification in the SHS samples. The AD SHS had higher aromaticity ($SUVA_{254}$) and extent of humification (HIX) than the FD SHS. The HHS had high $SUVA_{254}$, but the LHS had high HIX. The HIX had a significantly positive correlation with the ratio of $P_{III,n}/P_{II,n}$ which suggested that high humification of the LHS was attributed to the high extent of fulvic acid-like substance in the LHS. The size separation method successfully distinguished the chemical composition and structure of the size-fractioned SHS.

Supplementary Materials: The following are available online at https://www.mdpi.com/article/10.3390/app11178220/s1, Table S1: The optical indicators (S275-295, SR, A250-400, FI, and BIX) of size-fractioned SHS for AD and FD samples.

Author Contributions: Conceptualization, C.-W.C., W.-S.H. and T.-C.C.; methodology, C.-Y.H. and T.-C.C.; validation, W.-S.H.; formal analysis, W.-S.H. and Y.-Y.L.; writing—original draft preparation, C.-W.C. and T.-C.C.; writing—review and editing, C.-Y.H. and T.-C.C. All authors have read and agreed to the published version of the manuscript.

Funding: This work was supported by the National Pingtung University of Science and Technology, Taiwan.

Institutional Review Board Statement: Not applicable.

Informed Consent Statement: Not applicable.

Data Availability Statement: Data are available through the request to the corresponding author.

Conflicts of Interest: The authors declare no conflict of interest.

References

1. Chen, M.; Hur, J. Pre-treatments, characteristics, and biogeochemical dynamics of dissolved organic matter in sediments: A review. *Water Res.* **2015**, *79*, 10–25. [CrossRef] [PubMed]
2. Xu, H.; Guo, L. Intriguing changes in molecular size and composition of dissolved organic matter induced by microbial degradation and self-assembly. *Water Res.* **2018**, *135*, 187–194. [CrossRef] [PubMed]
3. Xu, H.; Zou, L.; Guan, D.; Li, W.; Jiang, H. Molecular weight-dependent spectral and metal binding properties of sediment dissolved organic matter from different origins. *Sci. Total Environ.* **2019**, *665*, 828–835. [CrossRef]
4. Burdige, D.J.; Komada, T. Sediment pore waters. In *Biogeochemistry of Marine Dissolved Organic Matter*; Elsevier: Amsterdam, The Netherlands, 2015; pp. 535–577.
5. He, W.; Chen, M.; Schlautman, M.A.; Hur, J. Dynamic exchanges between DOM and POM pools in coastal and inland aquatic ecosystems: A review. *Sci. Total Environ.* **2016**, *551*, 415–428. [CrossRef]
6. Hur, J.; Lee, D.-H.; Shin, H.-S. Comparison of the structural, spectroscopic and phenanthrene binding characteristics of humic acids from soils and lake sediments. *Org. Geochem.* **2009**, *40*, 1091–1099. [CrossRef]
7. Sun, W.; Ni, J.; Xu, N.; Sun, L. Fluorescence of sediment humic substance and its effect on the sorption of selected endocrine disruptors. *Chemosphere* **2007**, *66*, 700–707. [CrossRef] [PubMed]
8. Yamamoto, H.; Liljestrand, H.M.; Shimizu, Y.; Morita, M. Effects of physical−chemical characteristics on the sorption of selected endocrine disruptors by dissolved organic matter surrogates. *Environ. Sci. Technol.* **2003**, *37*, 2646–2657. [CrossRef]
9. Yeh, Y.-L.; Yeh, K.-J.; Hsu, L.-F.; Yu, W.-C.; Lee, M.-H.; Chen, T.-C. Use of fluorescence quenching method to measure sorption constants of phenolic xenoestrogens onto humic fractions from sediment. *J. Hazard. Mater.* **2014**, *277*, 27–33. [CrossRef]
10. Shi, M.-S.; Huang, W.-S.; Hsu, L.-F.; Yeh, Y.-L.; Chen, T.-C. Fluorescence of Size-Fractioned Humic Substance Extracted from Sediment and Its Effect on the Sorption of Phenanthrene. *Int. J. Environ. Res. Public Health* **2019**, *16*, 5087. [CrossRef]
11. Lee, Y.K.; Lee, M.-H.; Hur, J. A new molecular weight (MW) descriptor of dissolved organic matter to represent the MW-dependent distribution of aromatic condensation: Insights from biodegradation and pyrene binding experiments. *Sci. Total Environ.* **2019**, *660*, 169–176. [CrossRef]
12. Chin, Y.-P.; Aiken, G.R.; Danielsen, K.M. Binding of pyrene to aquatic and commercial humic substances: The role of molecular weight and aromaticity. *Environ. Sci. Technol.* **1997**, *31*, 1630–1635. [CrossRef]
13. Hur, J.; Park, M.-H.; Schlautman, M.A. Microbial transformation of dissolved leaf litter organic matter and its effects on selected organic matter operational descriptors. *Environ. Sci. Technol.* **2009**, *43*, 2315–2321. [CrossRef]
14. Zhang, F.; Yang, L.; Liu, X.; Li, Y.; Fang, H.; Wang, X.; Alharbi, N.S.; Li, J. Sorption of 17β-estradiol to the dissolved organic matter from animal wastes: Effects of composting and the role of fulvic acid-like aggregates. *Environ. Sci. Pollut. Res.* **2018**, *25*, 16875–16884. [CrossRef]
15. Chen, G.; Lin, C.; Chen, L.; Yang, H. Effect of size-fractionation dissolved organic matter on the mobility of prometryne in soil. *Chemosphere* **2010**, *79*, 1046–1055. [CrossRef]
16. McPhedran, K.N.; Seth, R.; Drouillard, K.G. Investigation of Hydrophobic Organic Carbon (HOC) partitioning to 1 kDa fractionated municipal wastewater colloids. *Environ. Sci. Technol.* **2013**, *47*, 2548–2553. [CrossRef]
17. Chuang, W.-C.; Hsu, L.-F.; Tsai, H.-C.; Liu, Y.-Y.; Huang, W.-S.; Chen, T.-C. Nickel Binding Affinity with Size-Fractioned Sediment Dissolved and Particulate Organic Matter and Correlation with Optical Indicators. *Appl. Sci.* **2020**, *10*, 8995. [CrossRef]
18. Hsieh, S.-H.; Chiu, T.-P.; Huang, W.-S.; Chen, T.-C.; Yeh, Y.-L. Cadmium (Cd) and Nickel (Ni) Distribution on Size-Fractioned Soil Humic Substance (SHS). *Int. J. Environ. Res. Public Health* **2019**, *16*, 3398. [CrossRef]
19. Hur, J.; Kim, G. Comparison of the heterogeneity within bulk sediment humic substances from a stream and reservoir via selected operational descriptors. *Chemosphere* **2009**, *75*, 483–490. [CrossRef]
20. Hur, J.; Lee, B.-M.; Shin, K.-H. Spectroscopic characterization of dissolved organic matter isolates from sediments and the association with phenanthrene binding affinity. *Chemosphere* **2014**, *111*, 450–457. [CrossRef] [PubMed]
21. Hu, B.; Wang, P.; Wang, C.; Qian, J.; Bao, T.; Shi, Y. Investigating spectroscopic and copper-binding characteristics of organic matter derived from sediments and suspended particles using EEM-PARAFAC combined with two-dimensional fluorescence/FTIR correlation analyses. *Chemosphere* **2019**, *219*, 45–53. [CrossRef]
22. Chen, W.; Westerhoff, P.; Leenheer, J.A.; Booksh, K. Fluorescence excitation−emission matrix regional integration to quantify spectra for dissolved organic matter. *Environ. Sci. Technol.* **2003**, *37*, 5701–5710. [CrossRef]
23. Derrien, M.; Yang, L.; Hur, J. Lipid biomarkers and spectroscopic indices for identifying organic matter sources in aquatic environments: A review. *Water Res.* **2017**, *112*, 58–71. [CrossRef]
24. Hansen, A.M.; Kraus, T.E.; Pellerin, B.A.; Fleck, J.A.; Downing, B.D.; Bergamaschi, B.A. Optical properties of dissolved organic matter (DOM): Effects of biological and photolytic degradation. *Limnol. Oceanogr.* **2016**, *61*, 1015–1032. [CrossRef]
25. He, X.; Xi, B.; Wei, Z.; Guo, X.; Li, M.; An, D.; Liu, H. Spectroscopic characterization of water extractable organic matter during composting of municipal solid waste. *Chemosphere* **2011**, *82*, 541–548. [CrossRef]
26. He, X.-S.; Xi, B.-D.; Wei, Z.-M.; Jiang, Y.-H.; Yang, Y.; An, D.; Cao, J.-L.; Liu, H.-L. Fluorescence excitation–emission matrix spectroscopy with regional integration analysis for characterizing composition and transformation of dissolved organic matter in landfill leachates. *J. Hazard. Mater.* **2011**, *190*, 293–299. [CrossRef]

27. Tian, W.; Li, L.; Liu, F.; Zhang, Z.; Yu, G.; Shen, Q.; Shen, B. Assessment of the maturity and biological parameters of compost produced from dairy manure and rice chaff by excitation–emission matrix fluorescence spectroscopy. *Bioresour. Technol.* **2012**, *110*, 330–337. [CrossRef]
28. Wang, Y.; Hu, Y.; Yang, C.; Wang, Q.; Jiang, D. Variations of DOM quantity and compositions along WWTPs-river-lake continuum: Implications for watershed environmental management. *Chemosphere* **2019**, *218*, 468–476. [CrossRef] [PubMed]
29. Xiao, K.; Yu, J.; Wang, S.; Du, J.; Tan, J.; Xue, K.; Wang, Y.; Huang, X. Relationship between fluorescence excitation-emission matrix properties and the relative degree of DOM hydrophobicity in wastewater treatment effluents. *Chemosphere* **2020**, *254*, 126830. [CrossRef] [PubMed]
30. He, X.-S.; Xi, B.-D.; Li, X.; Pan, H.-W.; An, D.; Bai, S.-G.; Li, D.; Cui, D.-Y. Fluorescence excitation–emission matrix spectra coupled with parallel factor and regional integration analysis to characterize organic matter humification. *Chemosphere* **2013**, *93*, 2208–2215. [CrossRef]
31. Tang, Z.; Yu, G.; Liu, D.; Xu, D.; Shen, Q. Different analysis techniques for fluorescence excitation–emission matrix spectroscopy to assess compost maturity. *Chemosphere* **2011**, *82*, 1202–1208. [CrossRef]
32. Hung, W.-N.; Lin, T.-F.; Chiu, C.-H.; Chiou, C.T. On the use of a freeze-dried versus an air-dried soil humic acid as a surrogate of soil organic matter for contaminant sorption. *Environ. Pollut.* **2012**, *160*, 125–129. [CrossRef]
33. Xu, G.; Sun, J.; Xu, R.; Lv, Y.; Shao, H.; Yan, K.; Zhang, L.; Blackwell, M. Effects of air-drying and freezing on phosphorus fractions in soils with different organic matter contents. *Plant Soil Environ.* **2011**, *57*, 228–234. [CrossRef]
34. Zhang, S.; Wang, S.; Shan, X.-Q. Effect of sample pretreatment upon the metal speciation in sediments by a sequential extraction procedure. *Chem. Speciat. Bioavail.* **2001**, *13*, 69–74. [CrossRef]
35. Swift, R.S. Organic matter characterization. In *Methods of Soil Analysis: Chemical Methods*; Soil Science Society American: Madison, WI, USA, 1996; Volume 5, pp. 1011–1069.
36. Helms, J.R.; Stubbins, A.; Ritchie, J.D.; Minor, E.C.; Kieber, D.J.; Mopper, K. Absorption spectral slopes and slope ratios as indicators of molecular weight, source, and photobleaching of chromophoric dissolved organic matter. *Limnol. Oceanogr.* **2008**, *53*, 955–969. [CrossRef]
37. Weishaar, J.L.; Aiken, G.R.; Bergamaschi, B.A.; Fram, M.S.; Fujii, R.; Mopper, K. Evaluation of specific ultraviolet absorbance as an indicator of the chemical composition and reactivity of dissolved organic carbon. *Environ. Sci. Technol.* **2003**, *37*, 4702–4708. [CrossRef]
38. Ohno, T. Fluorescence inner-filtering correction for determining the humification index of dissolved organic matter. *Environ. Sci. Technol.* **2002**, *36*, 742–746. [CrossRef]
39. Lapworth, D.J.; Kinniburgh, D. An R script for visualising and analysing fluorescence excitation–emission matrices (EEMs). *Comput. Geosci.* **2009**, *35*, 2160–2163. [CrossRef]
40. Matilainen, A.; Gjessing, E.T.; Lahtinen, T.; Hed, L.; Bhatnagar, A.; Sillanpää, M. An overview of the methods used in the characterisation of natural organic matter (NOM) in relation to drinking water treatment. *Chemosphere* **2011**, *83*, 1431–1442. [CrossRef]
41. Fei, Y.-H.; Li, X.-D.; Li, X.-Y. Organic diagenesis in sediment and its impact on the adsorption of bisphenol A and nonylphenol onto marine sediment. *Mar. Pollut. Bull.* **2011**, *63*, 578–582. [CrossRef]
42. Dabrin, A.; Roulier, J.-L.; Coquery, M. Colloidal and truly dissolved metal (oid) fractionation in sediment pore waters using tangential flow filtration. *Appl. Geochem.* **2013**, *31*, 25–34. [CrossRef]
43. Jarvie, H.; Neal, C.; Rowland, A.; Neal, M.; Morris, P.; Lead, J.; Lawlor, A.; Woods, C.; Vincent, C.; Guyatt, H. Role of riverine colloids in macronutrient and metal partitioning and transport, along an upland–lowland land-use continuum, under low-flow conditions. *Sci. Total Environ.* **2012**, *434*, 171–185. [CrossRef]
44. Town, R.M.; Filella, M. Size fractionation of trace metal species in freshwaters: Implications for understanding their behaviour and fate. *Rev. Environ. Sci. Biotechnol.* **2002**, *1*, 277–297. [CrossRef]
45. Xu, H.; Houghton, E.M.; Houghton, C.J.; Guo, L. Variations in size and composition of colloidal organic matter in a negative freshwater estuary. *Sci. Total Environ.* **2018**, *615*, 931–941. [CrossRef]
46. Fellman, J.B.; Spencer, R.G.; Hernes, P.J.; Edwards, R.T.; D'Amore, D.V.; Hood, E. The impact of glacier runoff on the biodegradability and biochemical composition of terrigenous dissolved organic matter in near-shore marine ecosystems. *Mar. Chem.* **2010**, *121*, 112–122. [CrossRef]
47. Li, P.; Hur, J. Utilization of UV-Vis spectroscopy and related data analyses for dissolved organic matter (DOM) studies: A review. *Crit. Rev. Environ. Sci. Technol.* **2017**, *47*, 131–154. [CrossRef]
48. Birdwell, J.E.; Engel, A.S. Characterization of dissolved organic matter in cave and spring waters using UV–Vis absorbance and fluorescence spectroscopy. *Org. Geochem.* **2010**, *41*, 270–280. [CrossRef]
49. Huguet, A.; Vacher, L.; Relexans, S.; Saubusse, S.; Froidefond, J.-M.; Parlanti, E. Properties of fluorescent dissolved organic matter in the Gironde Estuary. *Org. Geochem.* **2009**, *40*, 706–719. [CrossRef]
50. Bilal, M.; Jaffrezic, A.; Dudal, Y.; Le Guillou, C.; Menasseri, S.; Walter, C. Discrimination of farm waste contamination by fluorescence spectroscopy coupled with multivariate analysis during a biodegradation study. *J. Agric. Food Chem.* **2010**, *58*, 3093–3100. [CrossRef]
51. Zhao, Y.; Song, K.; Shang, Y.; Shao, T.; Wen, Z.; Lv, L. Characterization of CDOM of river waters in China using fluorescence excitation-emission matrix and regional integration techniques. *J. Geophys. Res. Biogeosci.* **2017**, *122*, 1940–1953. [CrossRef]

52. Li, X.; Xing, M.; Yang, J.; Zhao, L.; Dai, X. Organic matter humification in vermifiltration process for domestic sewage sludge treatment by excitation–emission matrix fluorescence and Fourier transform infrared spectroscopy. *J. Hazard. Mater.* **2013**, *261*, 491–499. [CrossRef]
53. Chiu, T.-P.; Huang, W.-S.; Chen, T.-C.; Yeh, Y.-L. Fluorescence characteristics of dissolved organic matter (DOM) in percolation water and lateral seepage affected by soil solution (SS) in a lysimeter test. *Sensors* **2019**, *19*, 4016. [CrossRef] [PubMed]
54. Wang, W.; Wang, S.; Jiang, X.; Zheng, B.; Zhao, L.; Zhang, B.; Chen, J. Differences in fluorescence characteristics and bioavailability of water-soluble organic matter (WSOM) in sediments and suspended solids in Lihu Lake, China. *Environ. Sci. Pollut. Res.* **2018**, *25*, 12648–12662. [CrossRef] [PubMed]